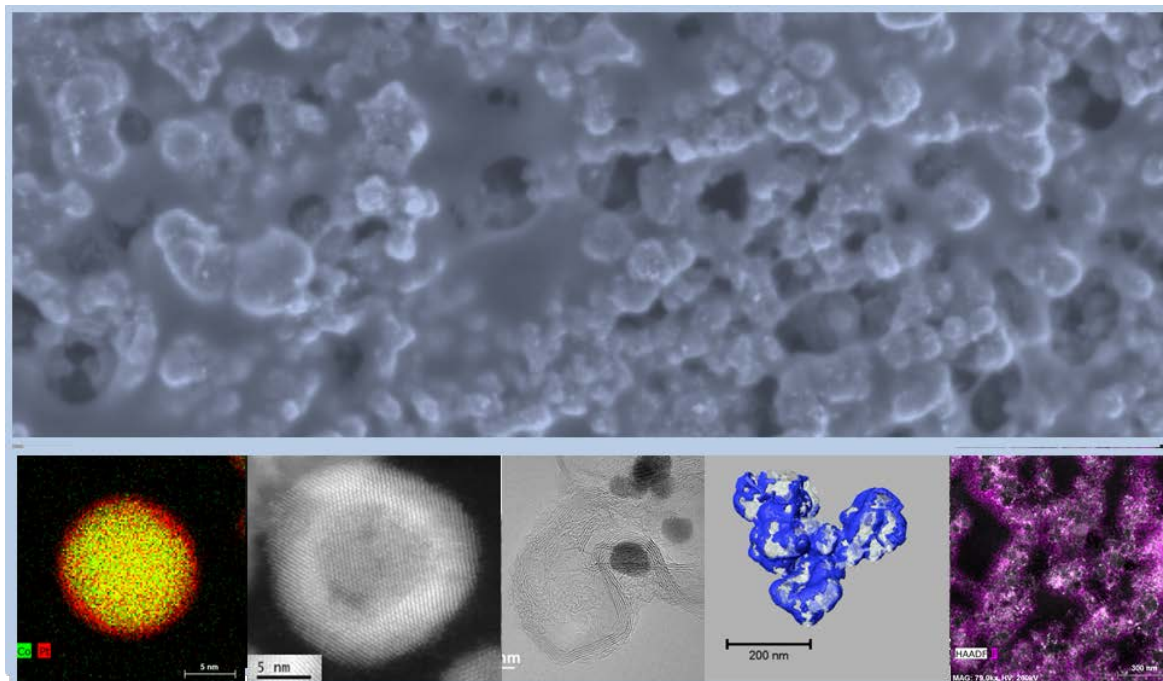


ADVANCED MICROSCOPY TECHNIQUES FOR STUDYING THE DURABILITY OF FUEL CELLS



Laure Guétaz, Sylvie Escibano, Fabrice Micoud
CEA-LITEN, Grenoble, France

The durability of PEMFCs remains, with their cost, one of the main barriers to the widespread commercialization of fuel-cell electric vehicles.



The first generation fuel cell vehicles (Toyota Mirai) have demonstrated their good performance:

- by using MEA with quite high Pt loading ($0.37 \text{ mg}_{\text{Pt}}/\text{cm}^2$)
- probably through the development of good system mitigation strategies

Borup et al., Current Opinion in Electrochemistry 2020, 21, 192

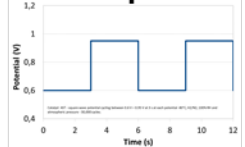
**To reduce the MEA Pt loading and to simplify the system management
⇒ it is crucial to still improve the durability of MEA components**

Two main strategies

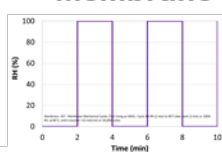
Ageing tests in single cell under accelerating stress test (AST) protocols



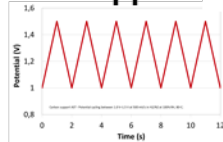
Pt nanoparticles



Membrane



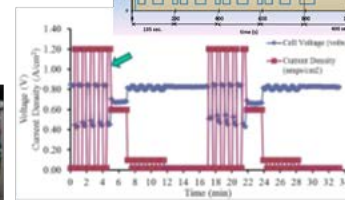
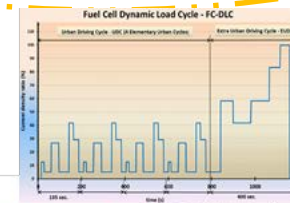
C support



https://energy.gov/sites/prod/files/2016/10/f33/fcto_myrd_d_fuel_cells.pdf

- Screening and selection of the MEA materials and components
- Accurate understanding of the degradation mechanisms of each component.

Ageing tests in stack under near real automotive application conditions



G. Tzotridis et al., EU Harmonised test protocols for PEMFC MEA testing in single cell configuration for automotive applications JRC Science for Policy report, 2015; EUR 27632 EN.

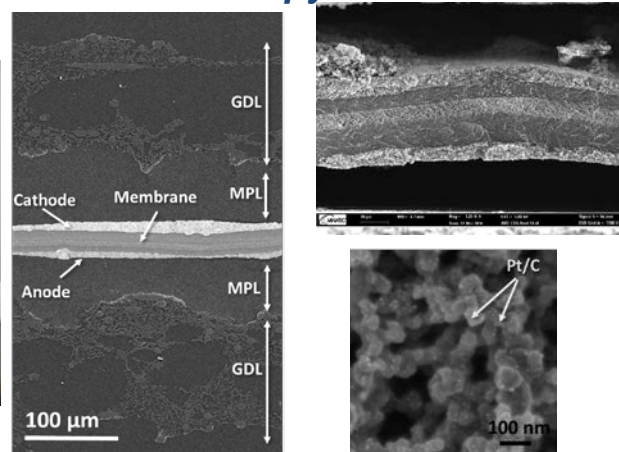
Stariha et al., JES, F492-501, 2018 & U. S. DoE "Fuel Cell Technologies Office Multi-Year Research, Development, and Demonstration Plan" (2016).
https://energy.gov/sites/prod/files/2016/10/f33/fcto_myrd_d_fuel_cells.pdf

- Which MEA components are degraded and by which mechanisms?
- Do the observed degraded components explain the performance losses?

Powerful tools to progress in degradation mechanisms understanding

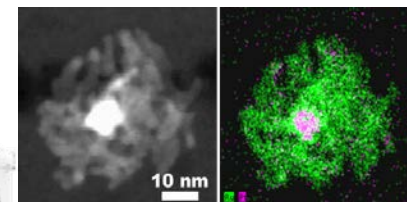
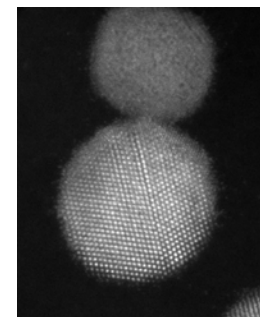
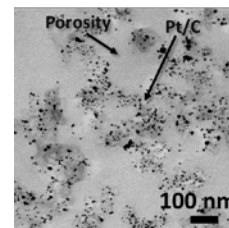
SEM

Scanning Electron Microscopy



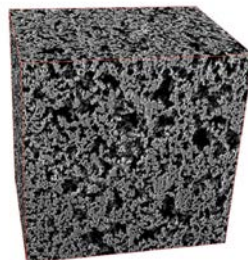
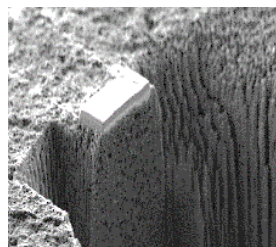
TEM

Transmission Electron Microscopy



FIB/SEM

Focused Ion Beam / Scanning Electron Microscopy-



Introduction

Pt and Pt alloy nanoparticle degradation

- Pt nanoparticles

 - Electrochemical Ostwald ripening: Pt nanoparticle growth

 - Pt membrane precipitation band

- Pt-Co nanoparticles

 - Electrochemical Ostwald ripening: Pt shell thickness increase

 - Ionomer contamination by Co cations

- Role of the carbon support

 - Pt nanoparticles can be localized on or inside the carbon

Carbon corrosion

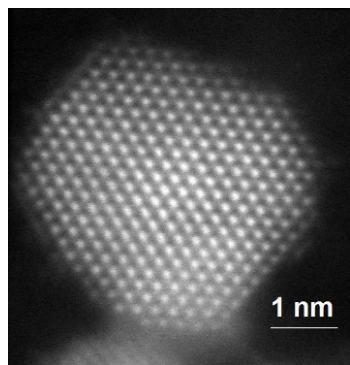
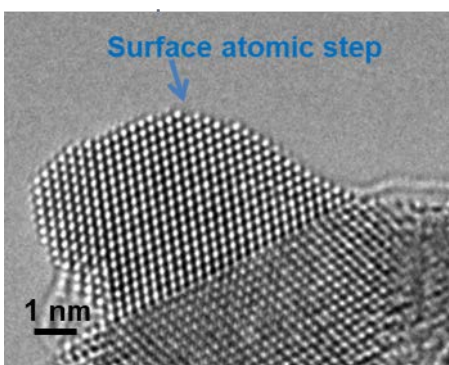
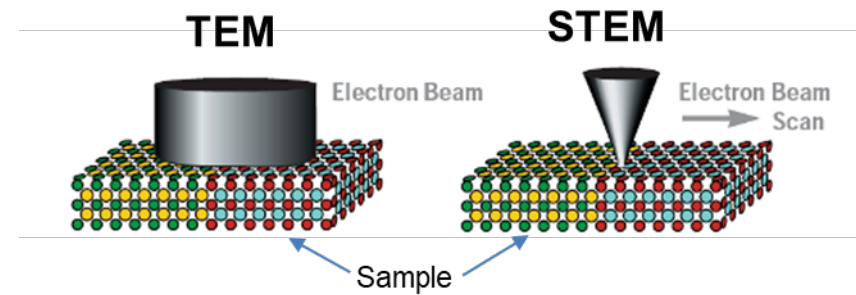
- Compaction of the cathode and effect on the Pt band localization

- Possibility to measure the porosity evolution by FIB-SEM

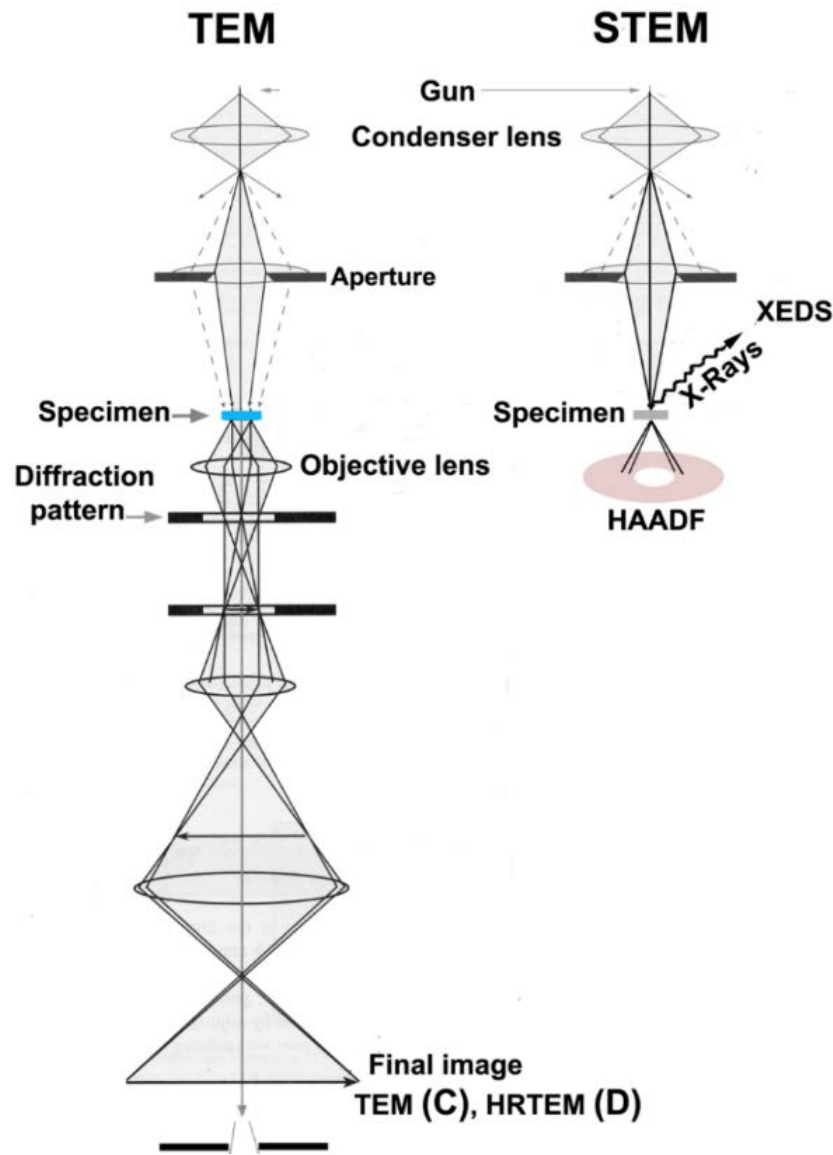
Membrane and cathode ionomer degradation

- Different locations of the membrane degradation

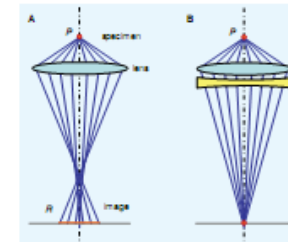
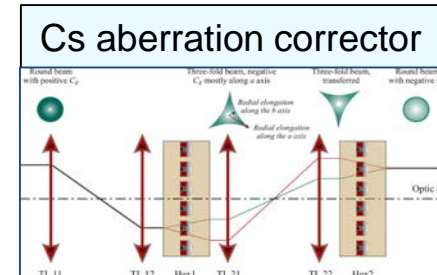
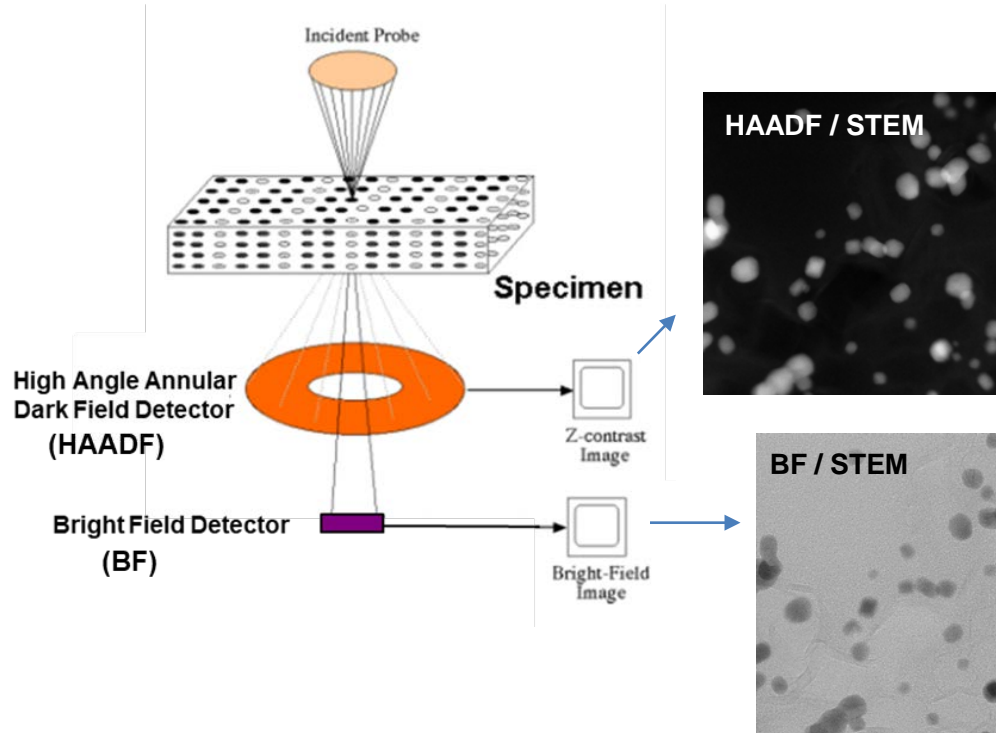
Conclusions



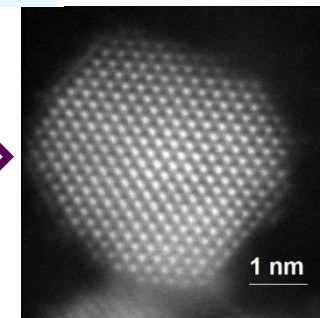
Atomic structure of Pt nanoparticles



HAADF / STEM



Atomic resolution

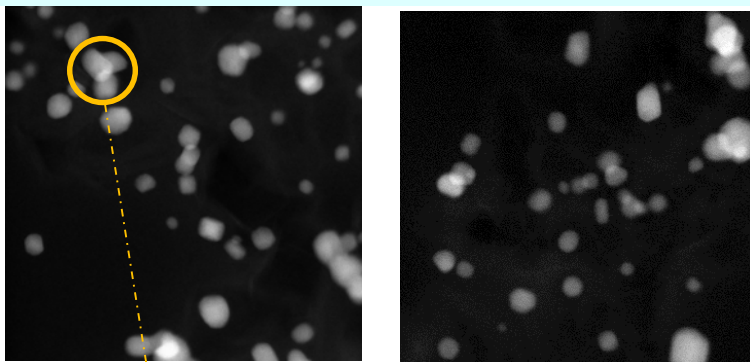


Advantages of HAADF/STEM

- **Chemical contrast (Z-contrast)**: heavier atoms scatter electrons more intensely than lighter atoms
- Possibility to analyze the **chemical composition of the atomic columns** during the scan by **EELS** or **X-EDS**

Nanoparticle size distribution is the main microstructural parameter

TEM or HAADF / STEM images



Nanoparticle size can be measured using image analysis software

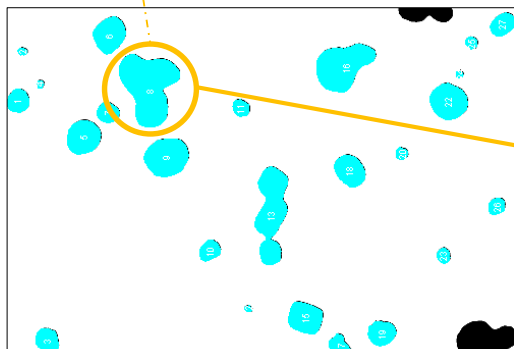
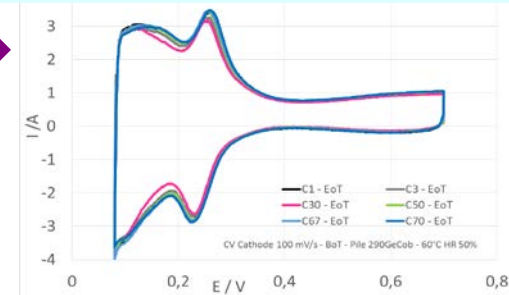


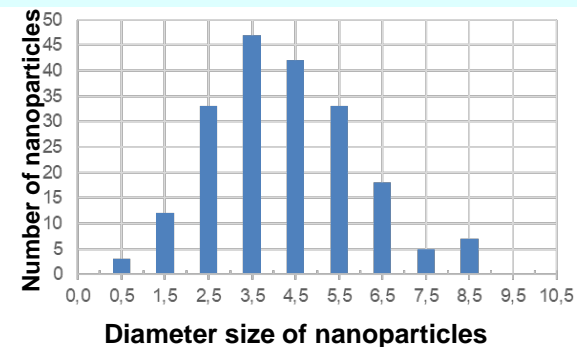
Image overlapping of nanoparticles that are not at the same level in the sample thickness is often measured as large nanoparticles → increase of the number of large nanoparticles

200 nanoparticles

Electrochemical Surface Area (ECSA)

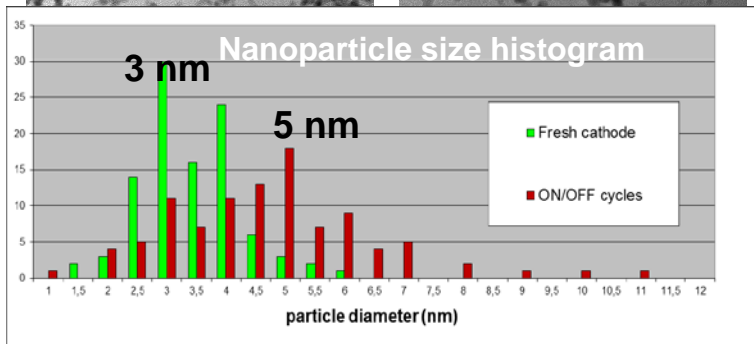
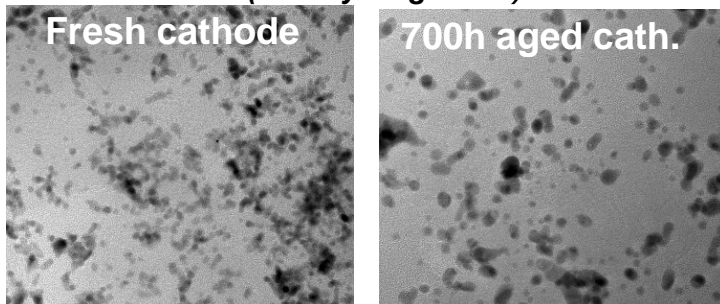


Nanoparticle size histogram



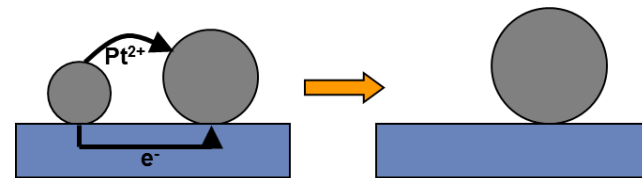
Nanoparticle size increases during fuel cell operation

Ageing tests representative of automotive application
(load cycling mode)



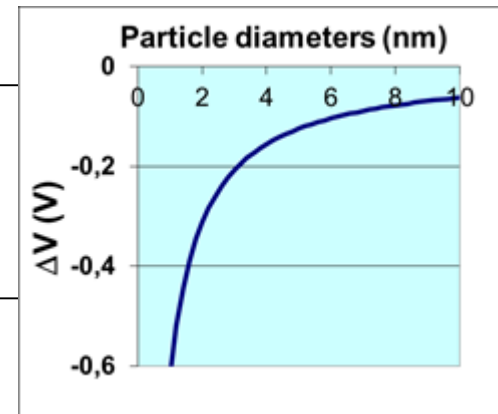
Pt surface area loss can be of 40-50% in few hundred hours of fuel cell operation time.

Electrochemical Ostwald ripening mechanism



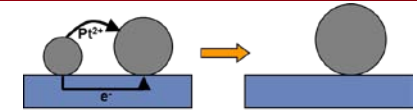
- ✓ Driven by the nanoparticle size dependence of the standard potential.

Negative shift in the standard electrode potentials of small nanoparticles (Plieth 1982)

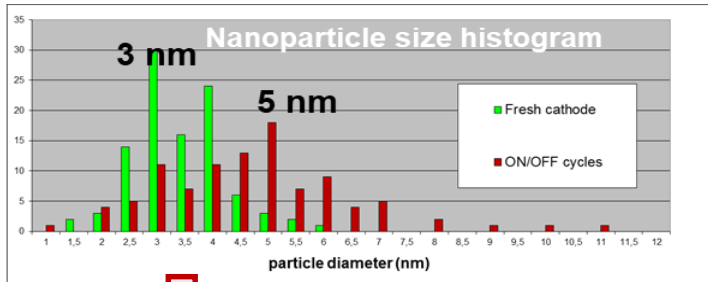


- ✓ Migration of Pt ions (and electron transfer) between neighboring nanoparticles.
- ✓ Enhanced by liquid water content due to higher ionomer ionic conduction.
- ✓ Slows down when nanoparticles become larger.

Particles with diameters ≥ 4.0 nm are stable



Electrochemical Ostwald ripening mechanism

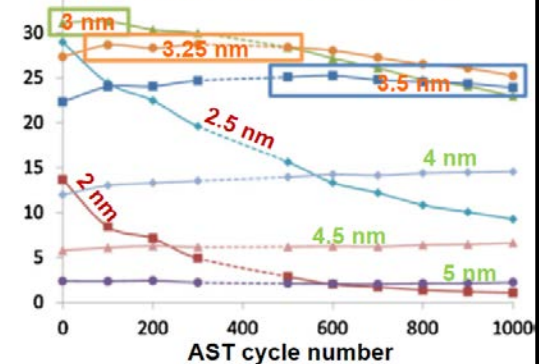
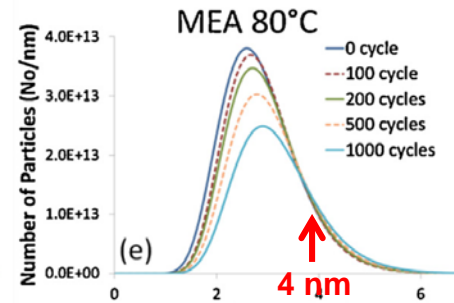


Evolution of Pt NP number for the different NP diameters

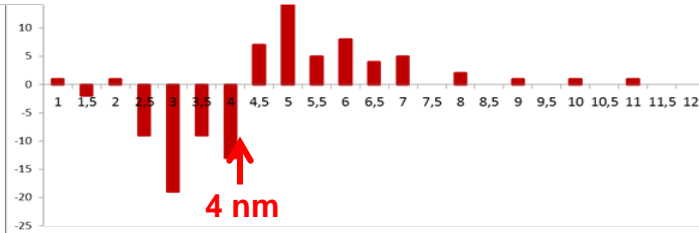
Similar results have been highlighted in studies performed by Operando A-SAXS during AST
(Gilbert et al., *Electrochimica Acta* 173, 2015, 223)

Nanoparticle size histogram evolution

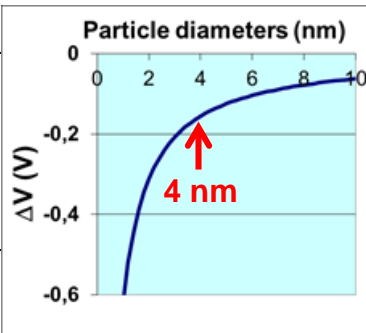
Evolution of Pt NP number during AST for different NP diameters



Aged Cathode Histogram – Fresh Cathode Histogram



Negative shift in the standard electrode potentials of small nanoparticles (Plieth 1982)



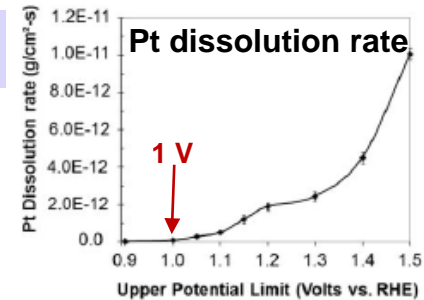
Optimization of the electrode microstructure by using larger nanoparticles (4-5 nm)

For potential larger than 1 V, a large amount of Pt is dissolved

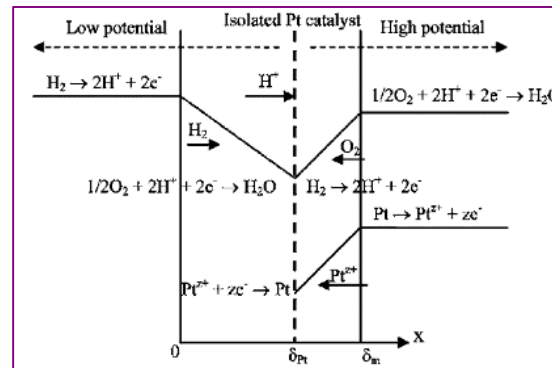
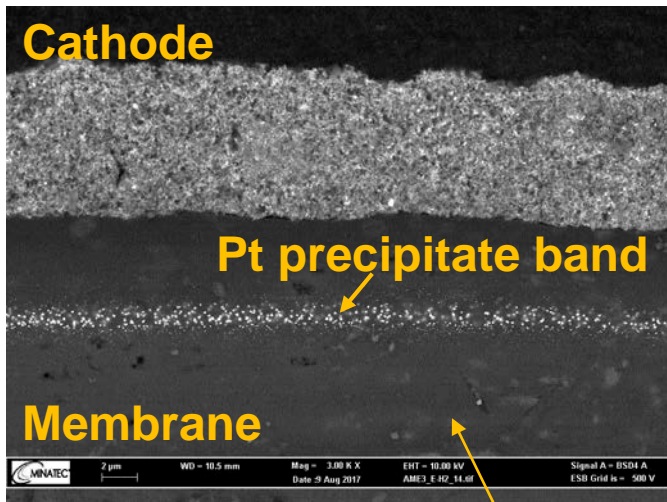
1. Pt ions migrate toward the membrane
2. Pt ions are reduced by H₂ crossover



Formation of a Pt precipitate band



Myers et al., *J. of Electrochem Soc.*, 165 (6), 2018, F3178



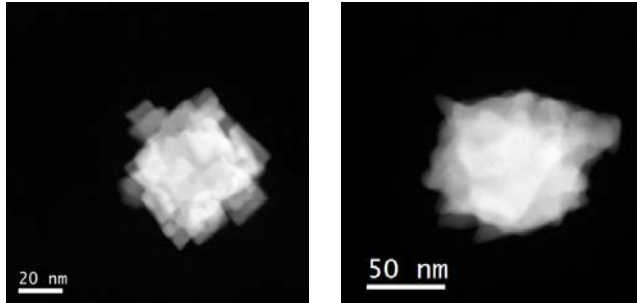
J. Zhang, *J. of Electrochem Soc.*, (2007), 154 (10) B1006.

- The position of this band depends on H₂/O₂ crossover.
- It is located where the crossover molar flux of O₂ equals one half of the crossover molar flux of H₂

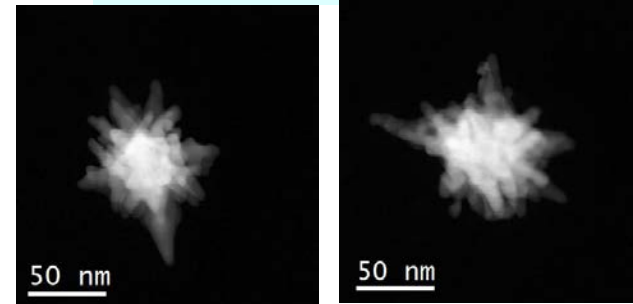
Small precipitates also appear in the whole area between the band and the anode.

The membrane Pt precipitates have different morphologies

Shape close to the cube



Star/dendritic shape



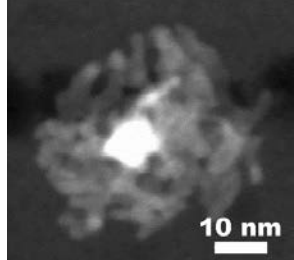
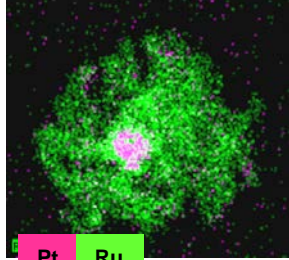
The precipitate shape probably results from the intensity fluxes of the Pt ions and/or H₂

(Ferreira et al. *Electrochemical and Solid-State Letters*, 10 3 2007, B60)



Lower Pt ion flux ⇒ shape close to the cube

Higher Pt ion flux ⇒ star/dendritic shape

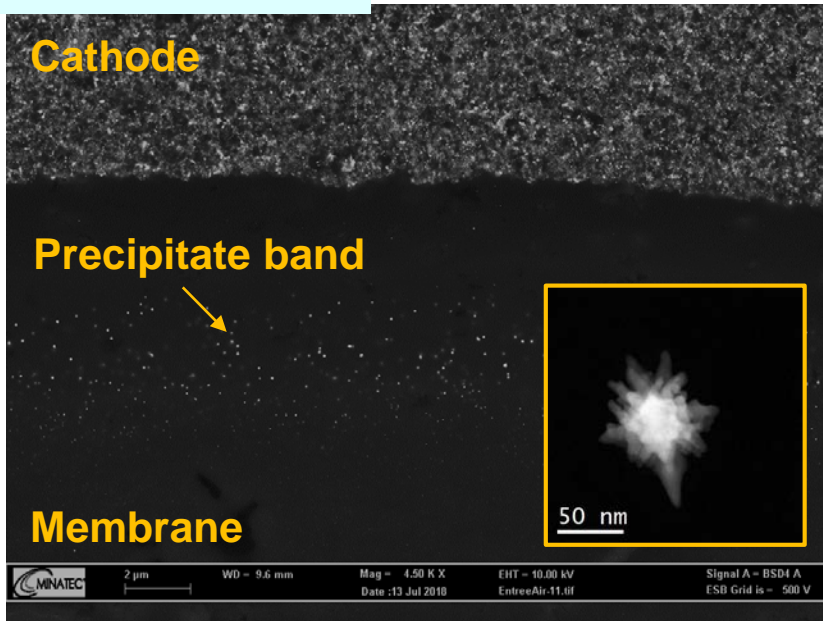




Star shaped precipitates are also observed when Pt-Ru anode is used: they are Pt-Ru precipitates

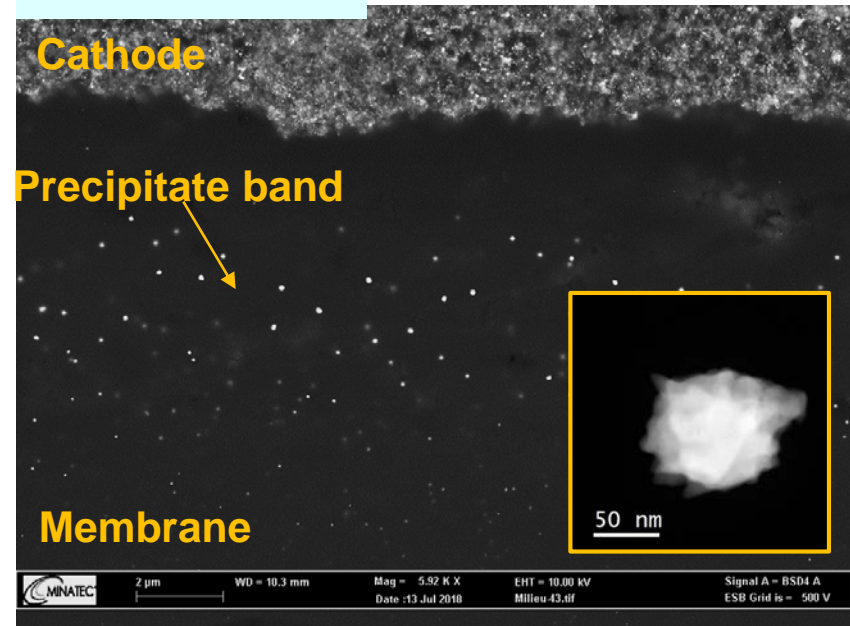
P.A. Henry et al., J. Power Sources 275 (2015) 312

The morphology of the membrane precipitates can provide some information on the MEA local conditions that could appear during the ageing test.

Air Inlet zone



Middle zone



The precipitate star/dendritic morphology indicates that probably a high-potential phase occurred during start/stop steps

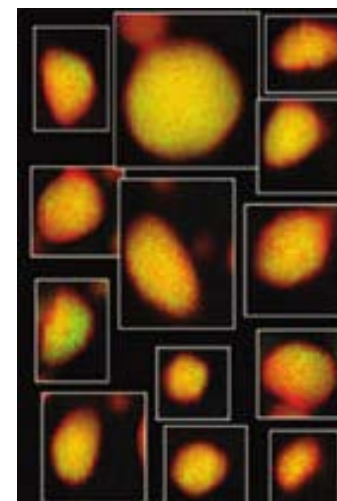
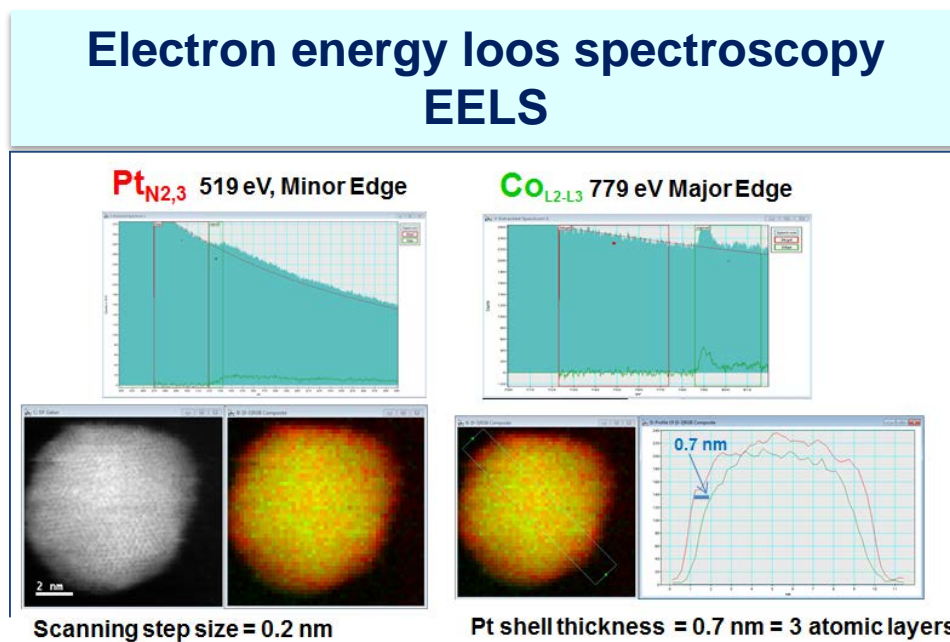
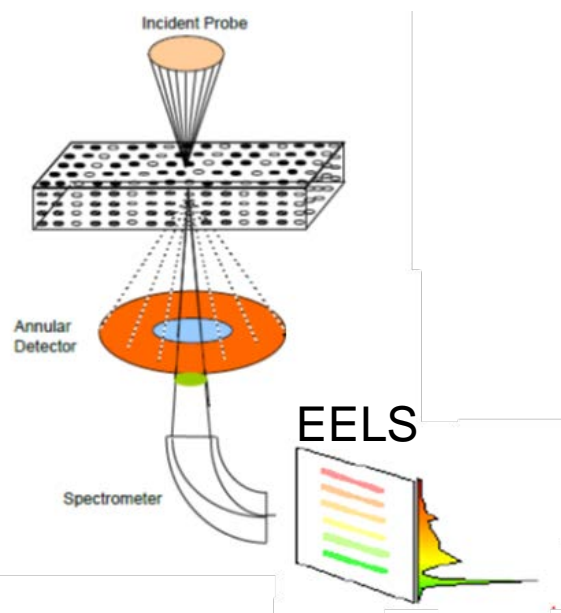
Pt alloys (Pt-Ni, Pt-Co): Higher Oxygen Reduction Reaction activity than pure Pt

Protection of the metal dissolution (*ionomer contamination*) by a Pt shell (acid leaching, heat treatment)



Chemical analysis at the atomic scale is needed

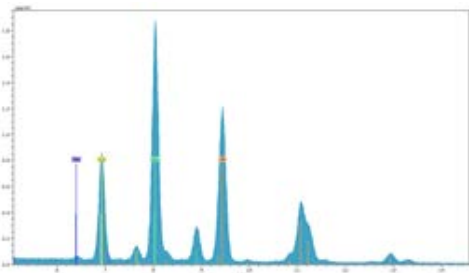
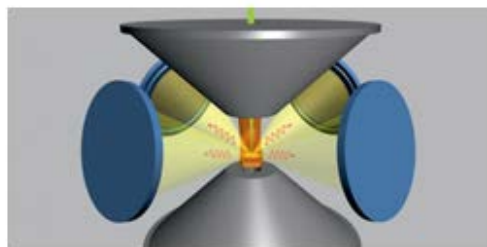
Electron energy loss spectroscopy EELS



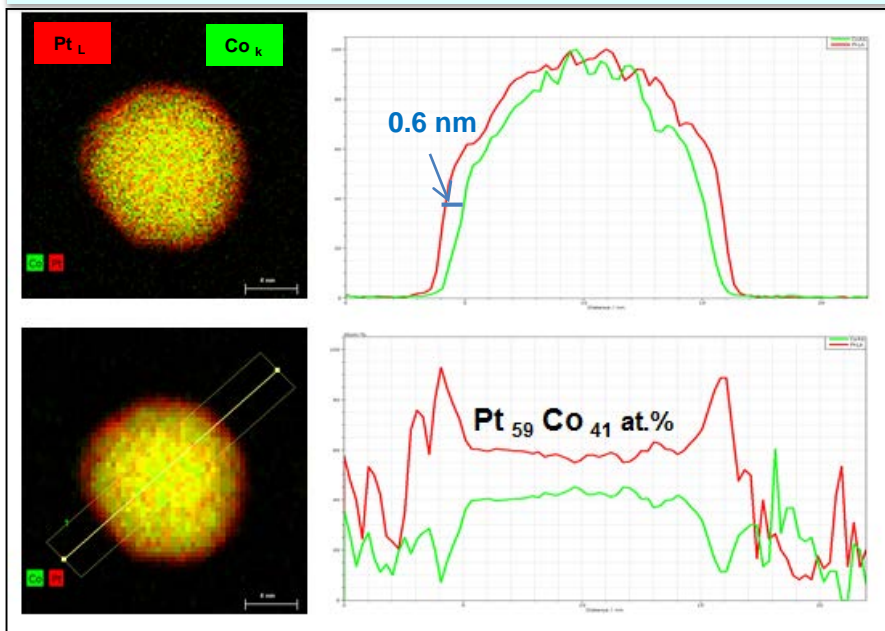
Xin et al., *Nano Lett.*
2012, 12, 1, 490



Chemical analysis at the atomic scale is needed

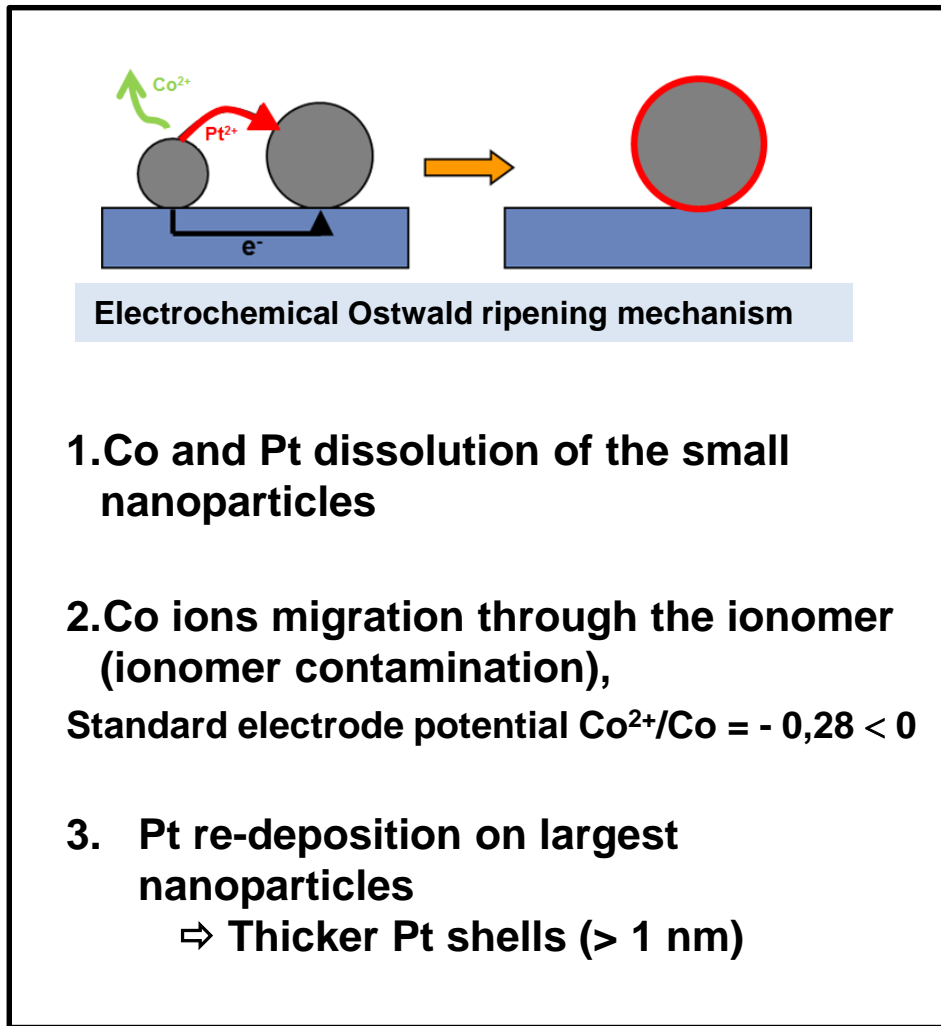
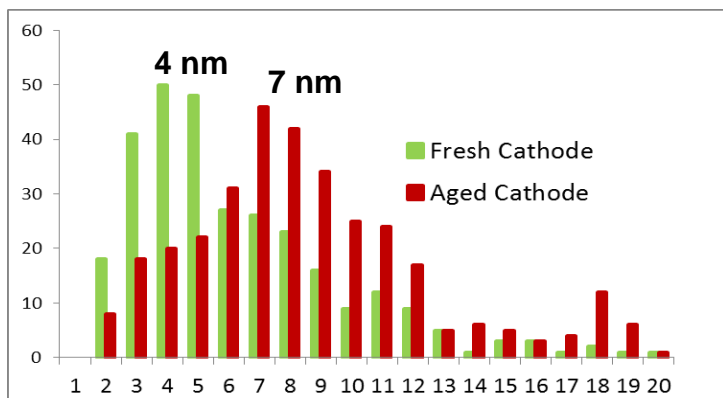
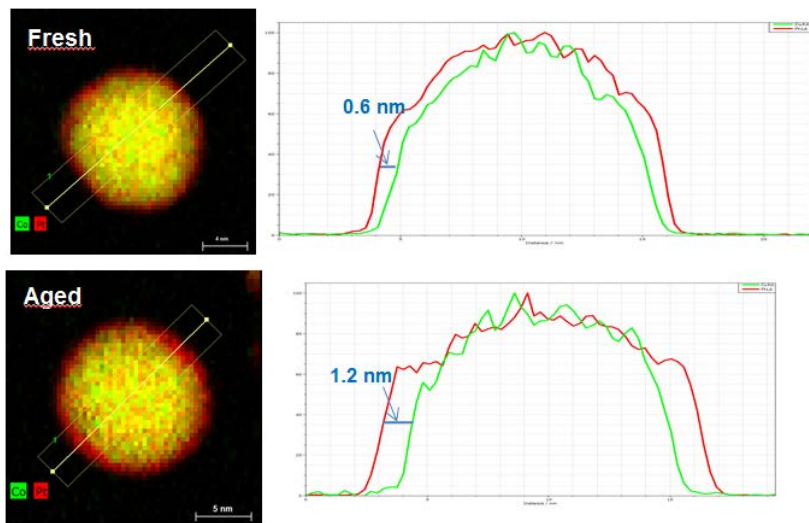


X-ray energy dispersion spectroscopy X-EDS



One nanoparticle X-EDS or EELS elemental map acquisition time: 5-10 min
 ► Difficulty to have statistically representative data when the catalysts are not homogeneous

Ageing tests representative of automotive application

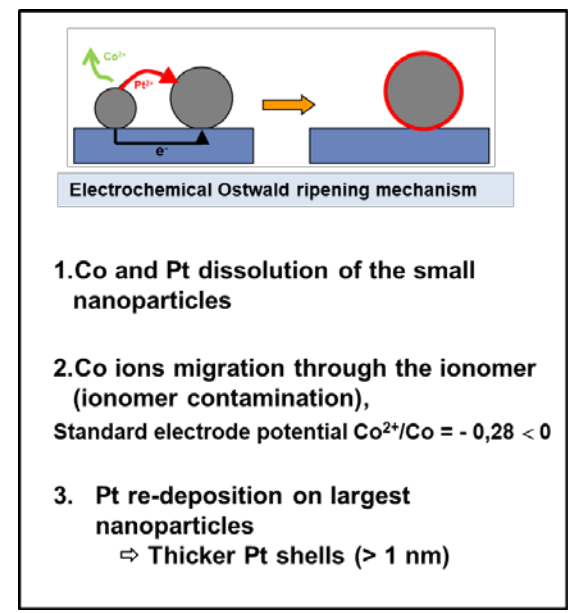
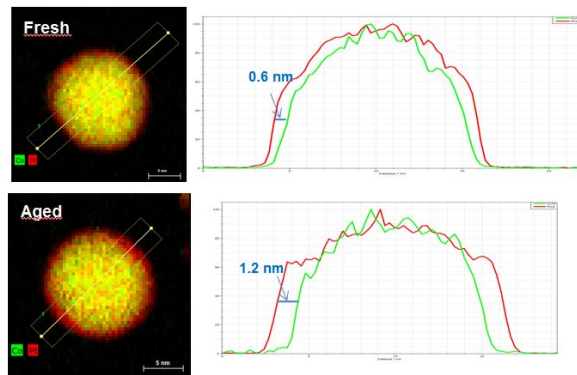
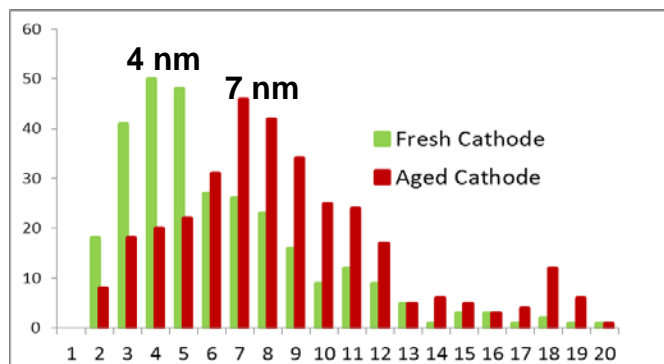


1. Co and Pt dissolution of the small nanoparticles
2. Co ions migration through the ionomer (ionomer contamination),
Standard electrode potential $\text{Co}^{2+}/\text{Co} = -0,28 < 0$
3. Pt re-deposition on largest nanoparticles
⇒ Thicker Pt shells (> 1 nm)

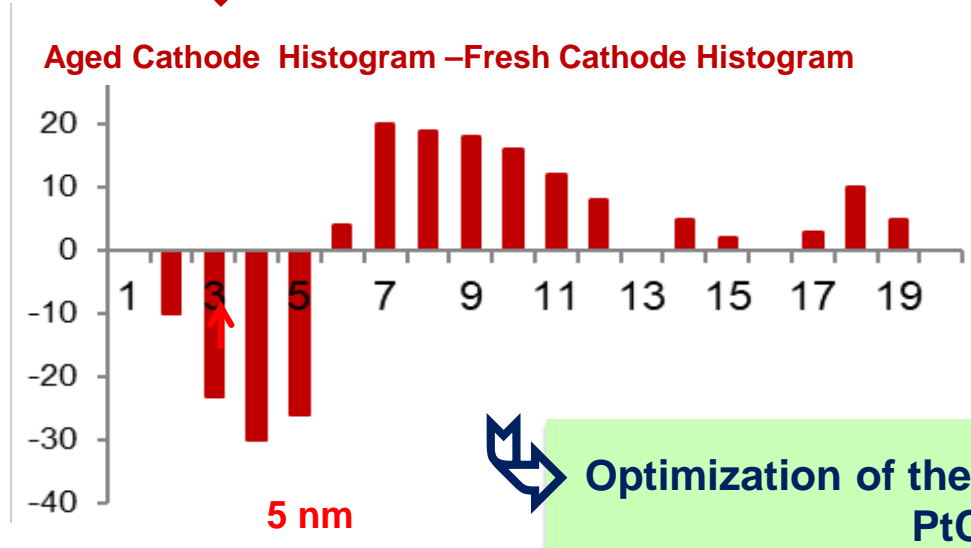


The electrochemical Ostwald ripening mechanism leads to thicker Pt shell surrounding the Pt-Co nanoparticles

Ageing tests representative of automotive application



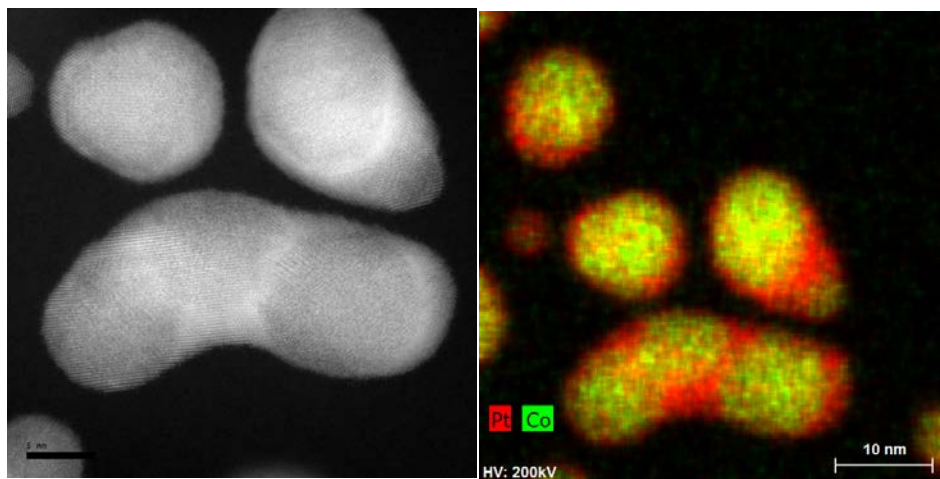
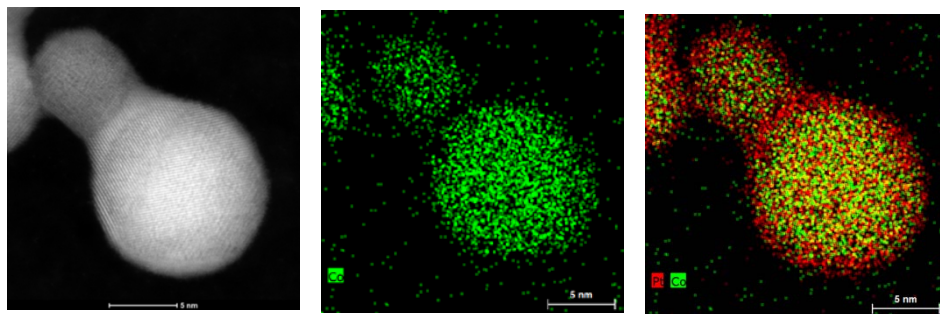
Evolution of Pt NP number for the different NP diameters



Nanoparticles smaller than 4-5 nm are dissolved (Pt shell is also dissolved)
Pt shell protects Co dissolution only for the larger nanoparticles

Optimization of the electrode microstructure by using larger PtCo nanoparticles (4-5 nm)

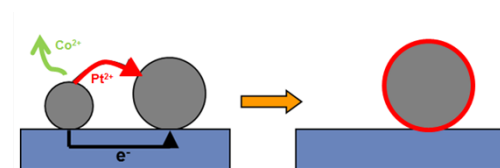
Pt re-deposition on neighboring Pt-Co nanoparticles leads to their coalescence



Nanoparticle sintering by Pt re-deposition

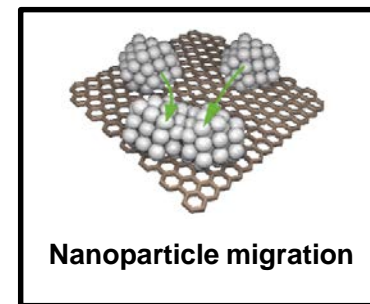


Coalescence of neighboring NP appears to result from Pt re-deposition rather than from nanoparticle migration



Electrochemical Ostwald ripening mechanism

1. Co and Pt dissolution of the small nanoparticles
2. Co ions migration through the ionomer (ionomer contamination),
Standard electrode potential $\text{Co}^{2+}/\text{Co} = -0,28 < 0$
3. Pt re-deposition on largest nanoparticles
⇒ Thicker Pt shells (> 1 nm)

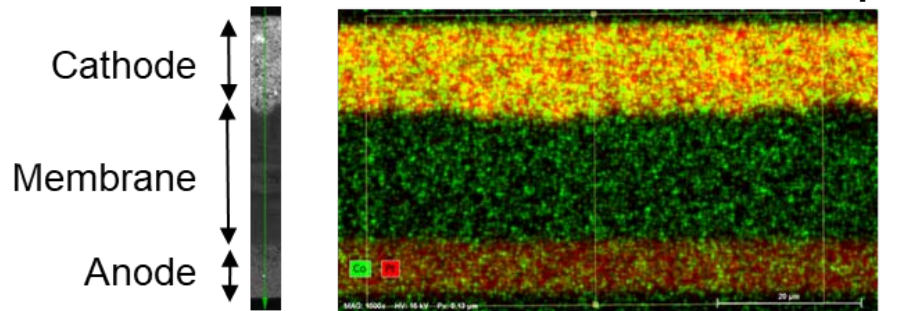


Nanoparticle migration

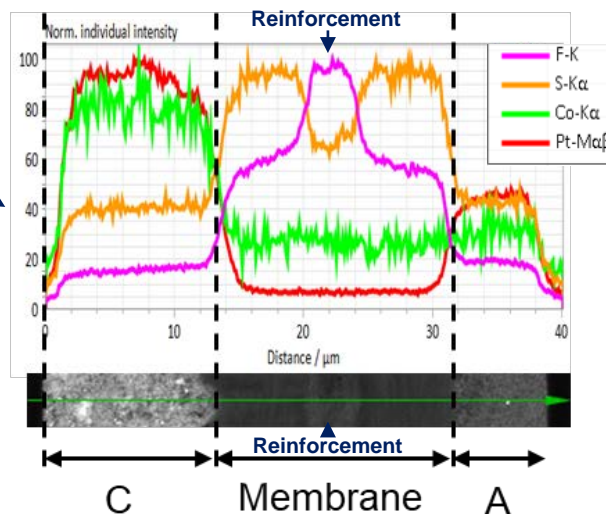
As the standard electrode potential of $\text{Co}^{2+}/\text{Co} < 0 \text{ V}$, the released Co cations remain in the ionomer
 Contrary to the Pt ions, Co ions are not reduced within the MEA.

Fresh MEA

Pt and Co X-EDS elemental maps



Lines scan across the MEA



The membrane contamination can be detected on MEA cross-section by X-EDS analysis in a SEM



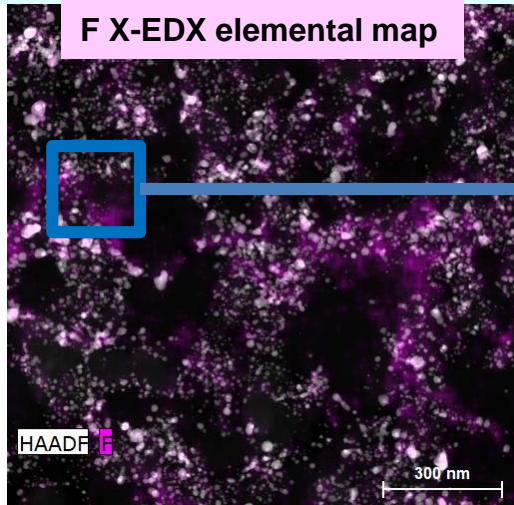
In order to avoid the contamination of the membrane during the sample preparation, the embedded cross-section was cut by microtomy in dry conditions



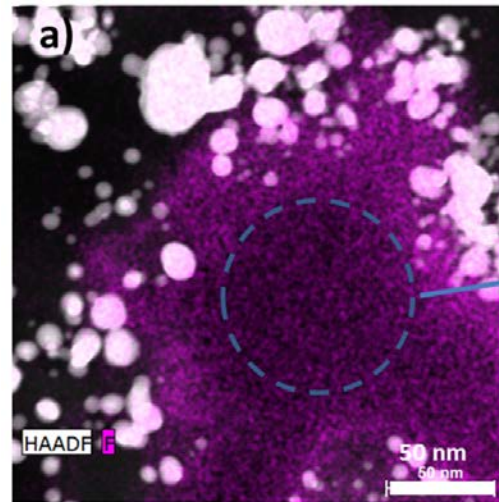
No Co cation are detected in the membrane of the fresh MEA

The ionomer in the cathode could be even more contaminated by Co cations than the membrane

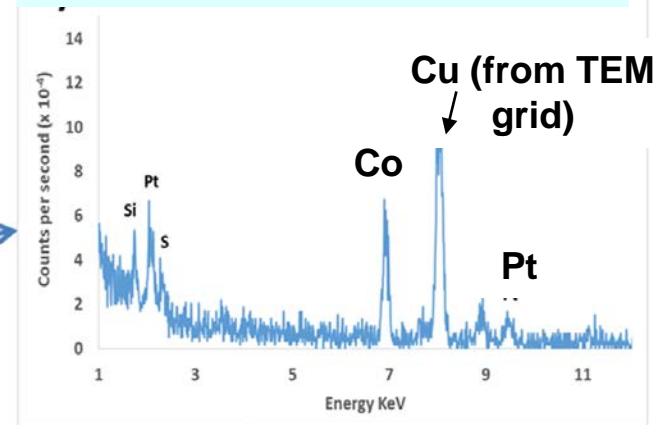
HAADF/STEM image of the cathode



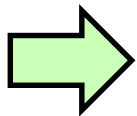
Pore filled with Nafion



EDS spectrum in the pore filled with Nafion



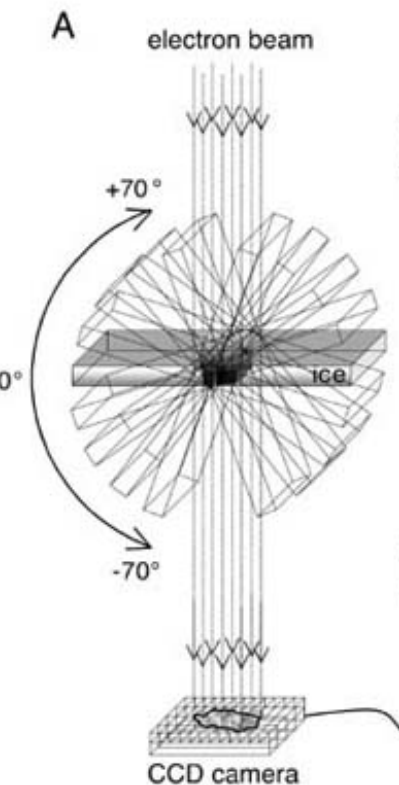
Large amount of Co is detected in the pore filled with Nafion



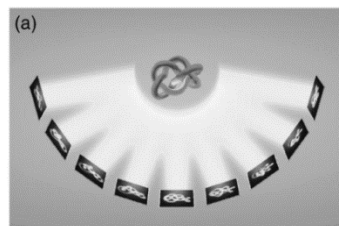
To reduce the ionomer contamination, it is important to lower the Co content in the catalysts (~10 at.% Co instead of 25 at.%)

Borup et al., Current Opinion in Electrochemistry 2020, 21, 192

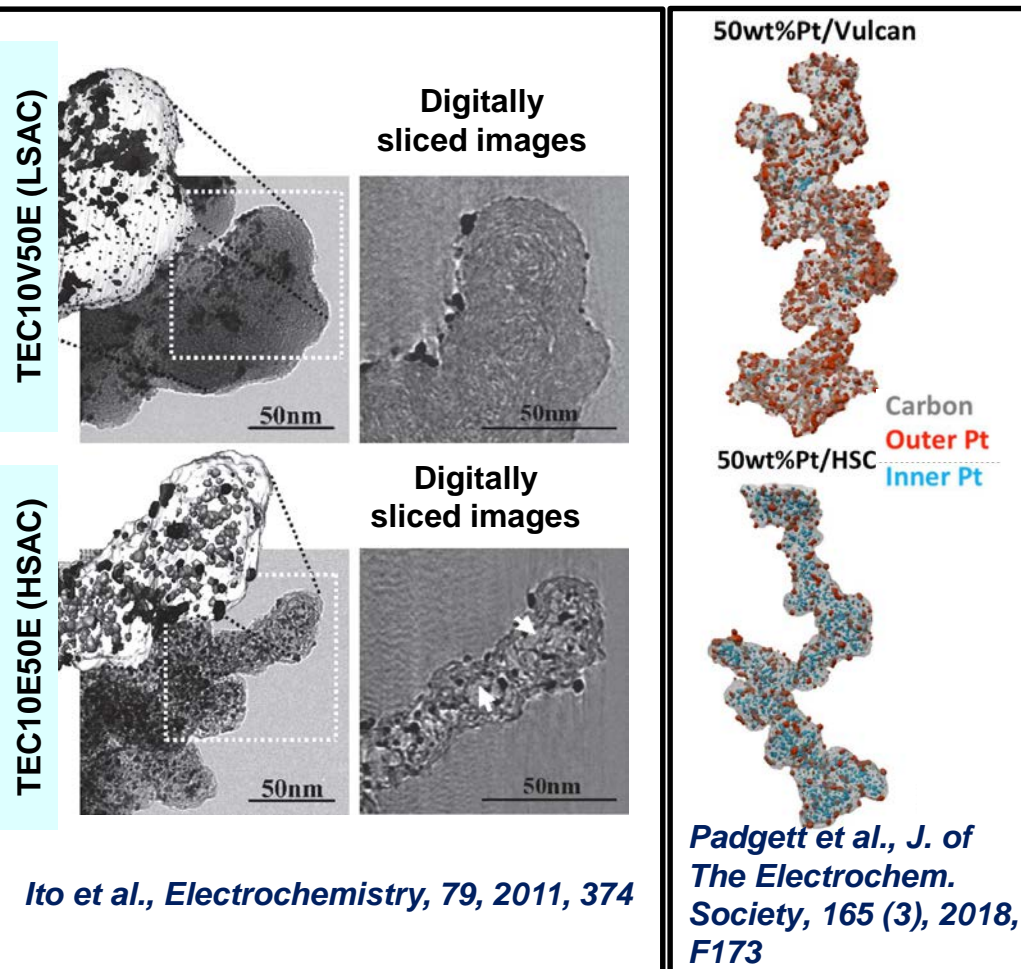
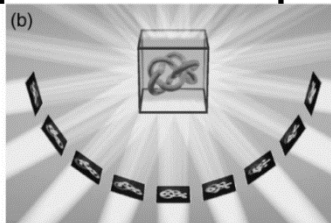
Electron tomography analyses have shown that for the high surface area carbon (HSAC) support, many nanoparticles are located inside the carbon



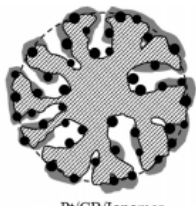
Tilt series of images is recorded



3D structure of the specimen is computed



The interior nanoparticles appear to be active, however they could be more sensitive to the local conditions (RH, current...)

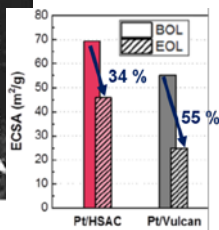
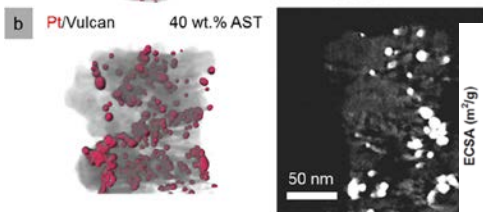
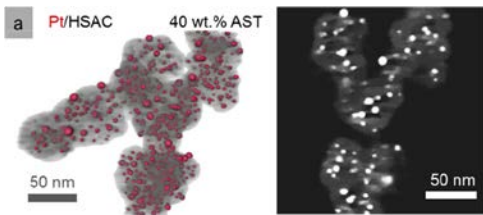


Nanoparticles in the interior of the CB are:

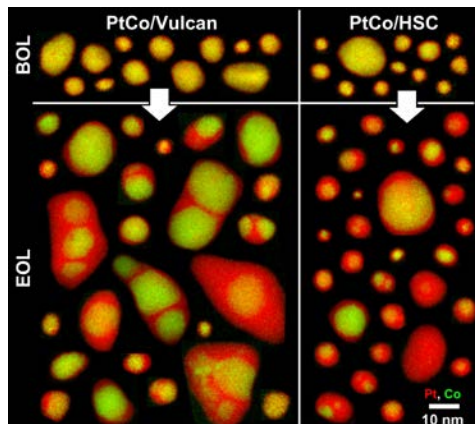
- ✓ active in low current density region
- ✓ no active in the high current density region due to their too low proton and O₂ accessibility

Park et al., J. Power Sources 315 (2016), 179

Are the interior nanoparticles less sensitive to coarsening ?



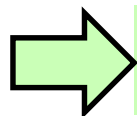
Sneed et al., ACS Appl. Mater. Interfaces, 9, 29839 (2017).



Padgett et al., J. of The Electrochem. Society, 166, 2019, (4) F198

➤ First studies suggest that the confinement of nanoparticles in C pores reduces the coalescence of neighboring nanoparticles

➤ It is yet not known whether their coarsening by the electrochemical Ostwald ripening is also limited

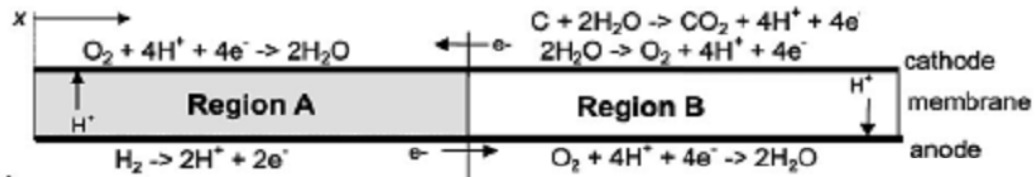


The optimization of carbon supports seems to be a promising path for the development of more efficient and resistant catalysts.

Carbon corrosion is often occurred during the start/stop procedure

During start/stop procedure, the anode can be partially exposed locally to O₂ creating a H₂ / O₂ front.

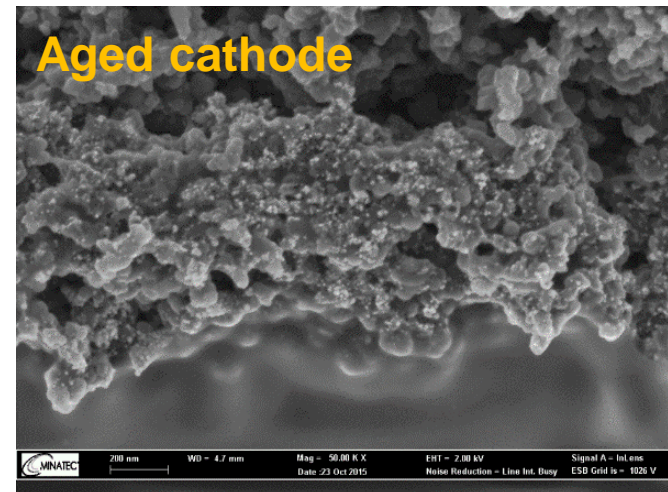
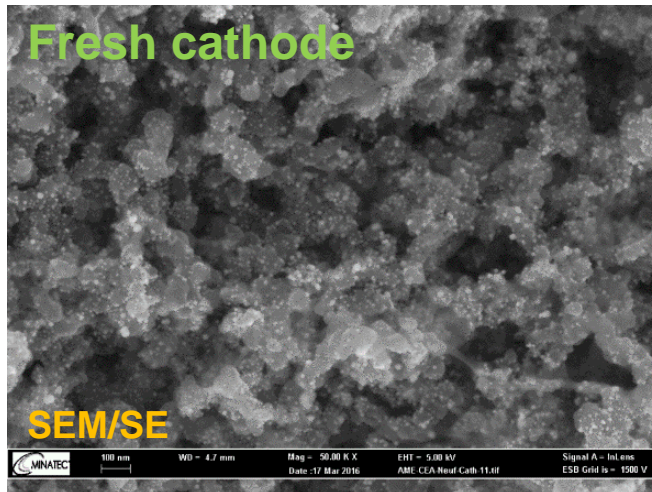
⇒ reverse current mechanism proposed by *Reiser (2005), Electrochemical and Solid-State Letters*, 8 (6) A273.



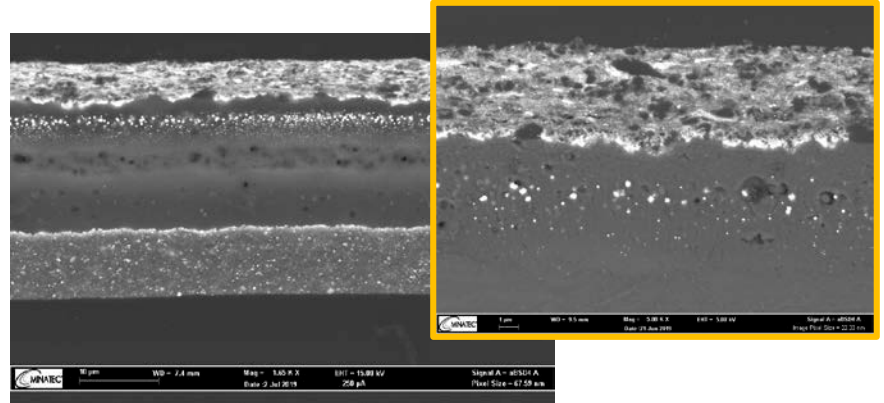
The high cathode potential leads to the carbon corrosion



Compaction of the cathode



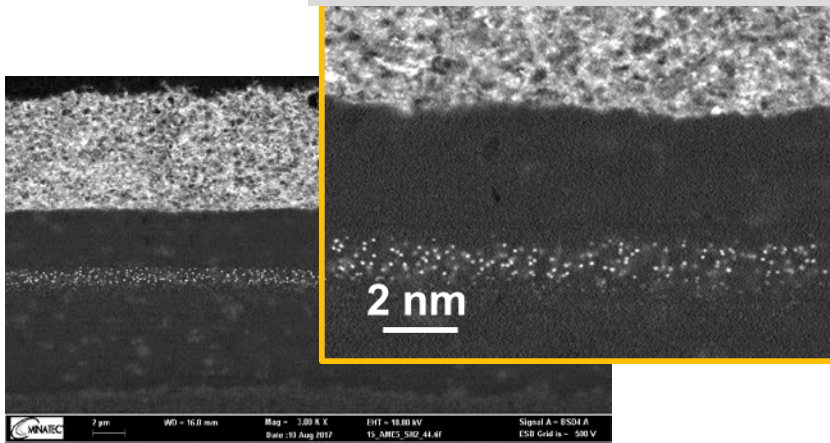
Carbon corrosion can modify the aspect of the cathode catalyst layer



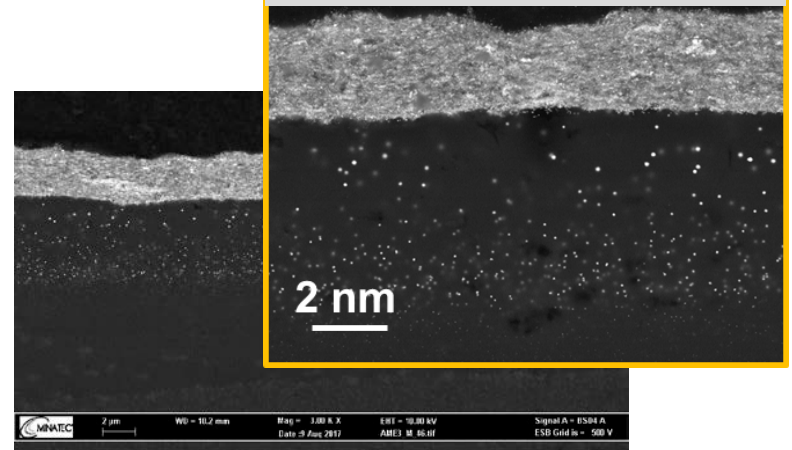
Carbon corrosion can change the position of the membrane Pt band

- Pt precipitates closer to the cathode revealing the presence of H₂ nearby the cathode / membrane interface
- That indicates that no more O₂ could diffuse into the membrane due to cathode compaction.

Cathode without compaction



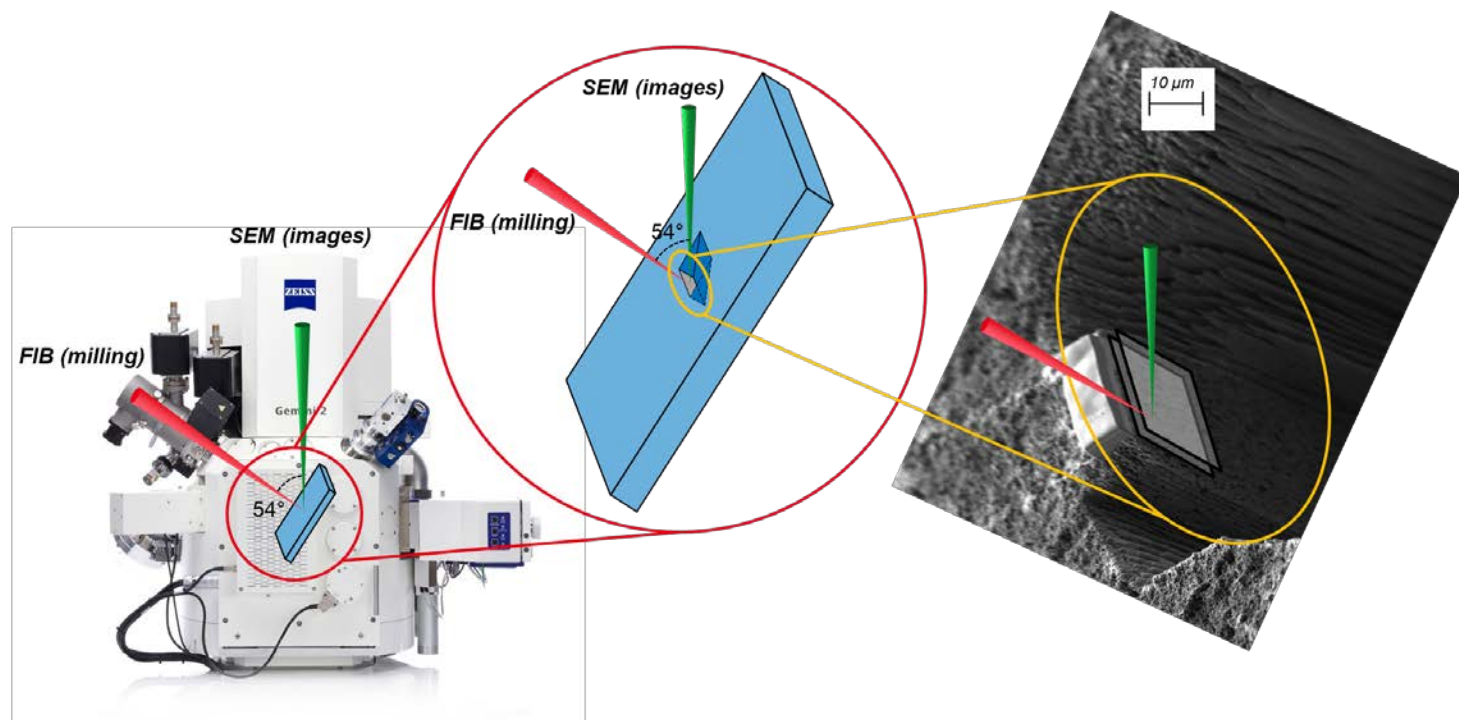
Compaction of the cathode

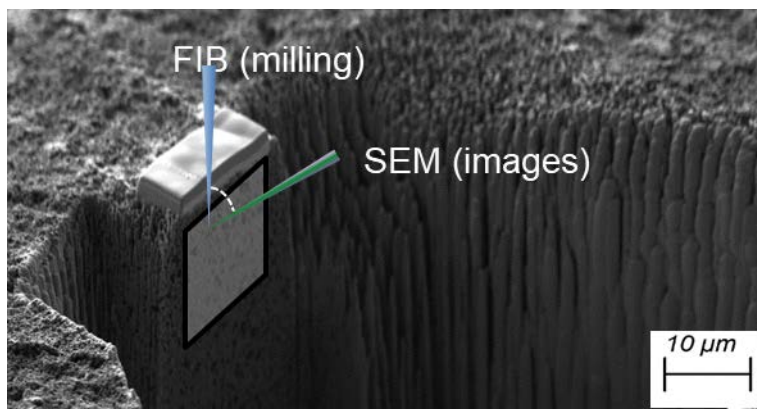


FIB/SEM

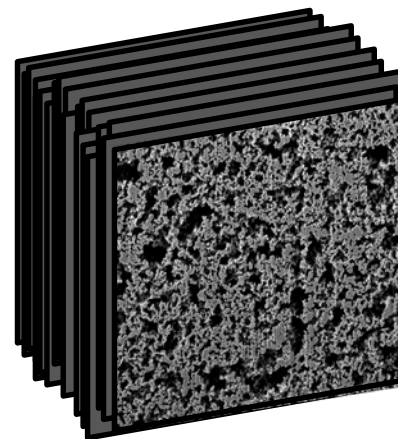
Focused Ion Beam / Scanning Electron Microscopy

Cathode compaction can be analyzed quantitatively by measuring the evolution of cathode porosity

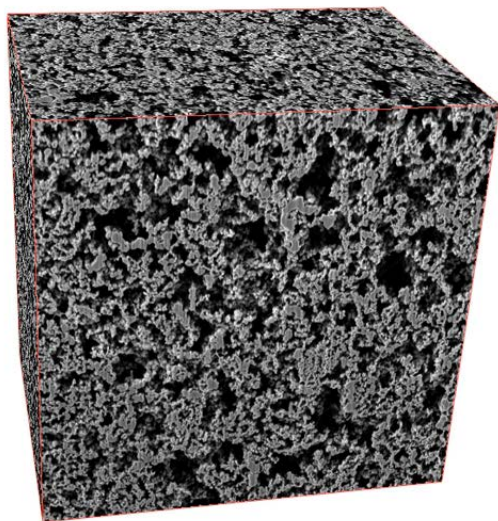




Stack of SEM images



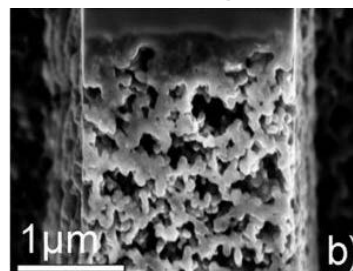
3D reconstruction of the MPL structure



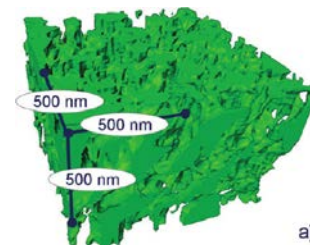
Courtesy of Thomas David, CEA-Liten

Fresh Cathode

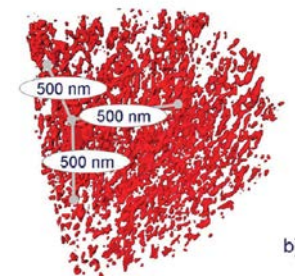
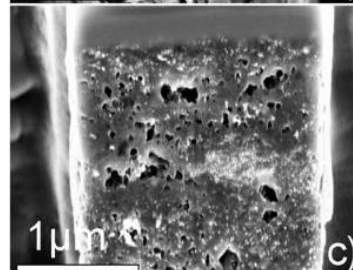
SEM images



Porosity analysis

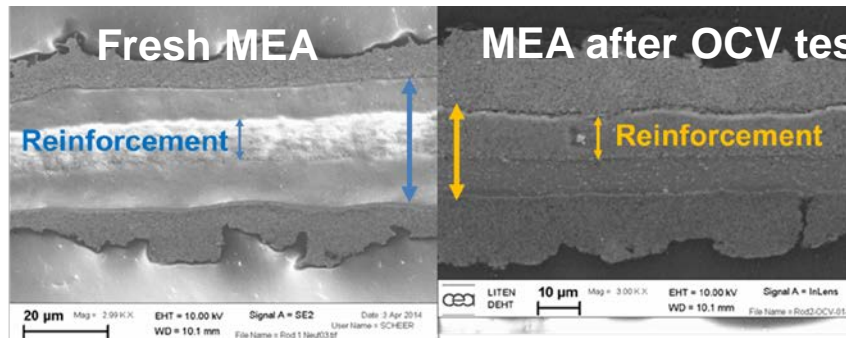


After 1000 cycles start-up/shut-down

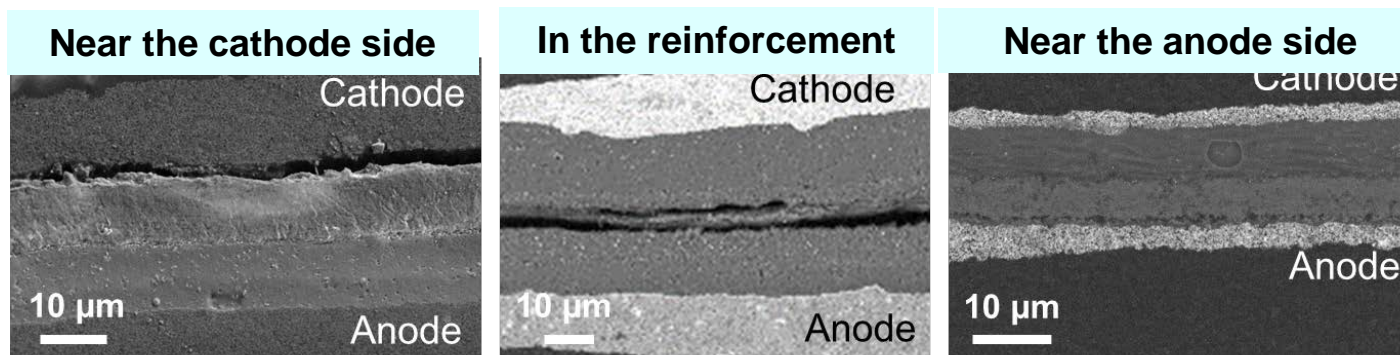


Schulenburg et al., J. Phys. Chem. C 2011, 115, 14236

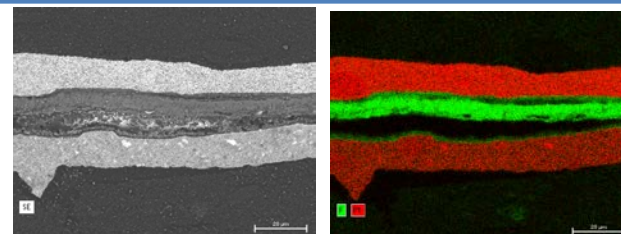
Degradation of the membrane, when it is severe, is visible on SEM MEA cross-sections



Membrane degradation can occur at different locations

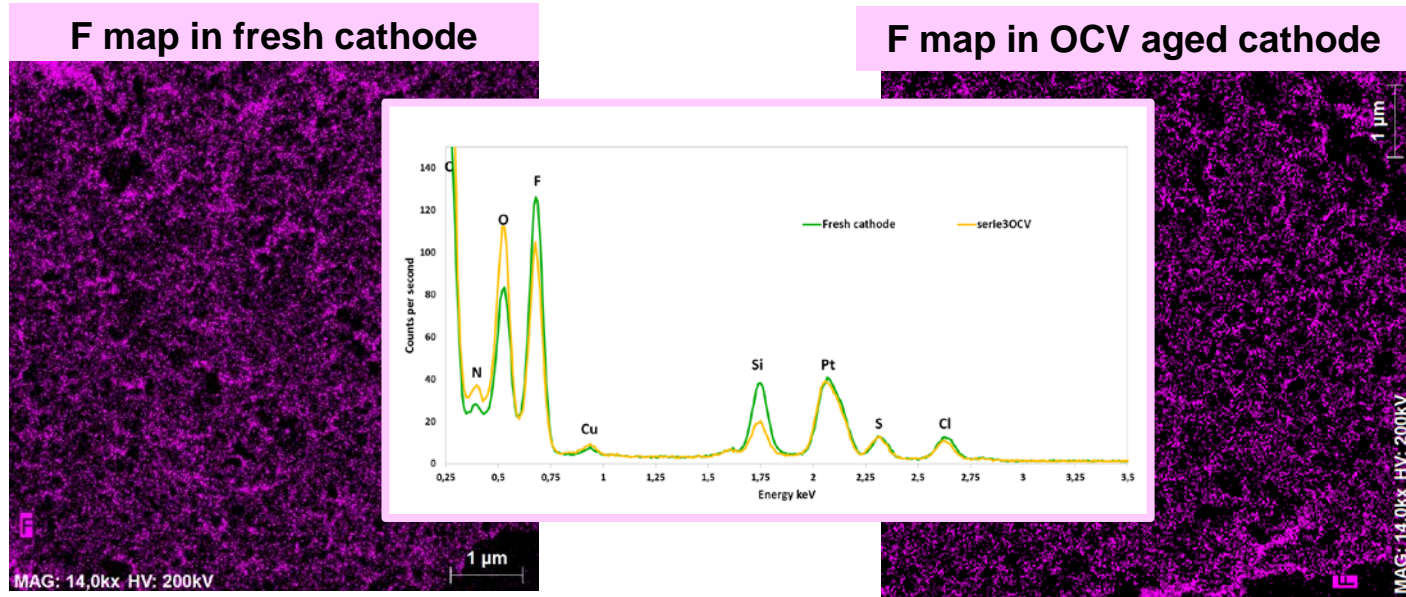


The epoxy resin can fill the voids left by the membrane degradation : light contrast between membrane and epoxy resin



Comparison of F content in the fresh and aged cathodes

Fluorine EDS elemental maps are acquired using low electron dose at cryogenic temperature



➔ No degradation of the Nafion is detected in the cathode aged under OCV conditions, even if severe membrane degradation was observed

Collaboration with Rod Borup (LANL)

To answer the question:

➤ **Which MEA components are degraded and by which mechanisms?**

The different electron microscopy techniques are powerful as they provide accurate analyses of the different MEA components and of their evolution after the ageing tests

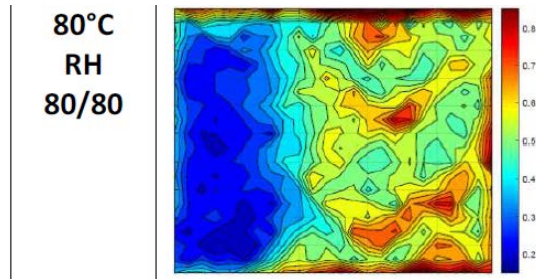
- ✓ **Pt and Pt alloys nanoparticles degradation by the electrochemical Ostwald ripening mechanism**
- ✓ **Pt dissolution and precipitate band in the membrane**
- ✓ **Contamination of the ionomer by the Co cations**
- ✓ **Distribution of the nanoparticles on or in the carbon support**
- ✓ **Deterioration of the cathode porosity by the carbon corrosion**
- ✓ **Severe membrane degradations**

However, to answer the question:

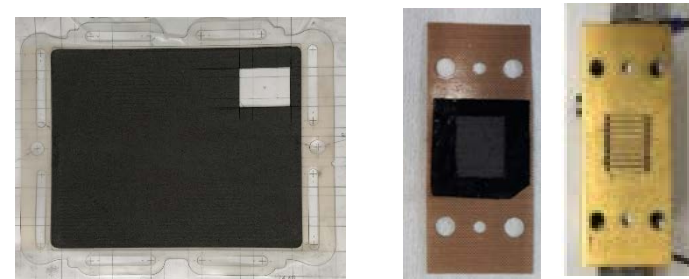
- Do the observed degraded components explain the performance losses?

Electron microscopy analyses must be combined with other local analyses techniques

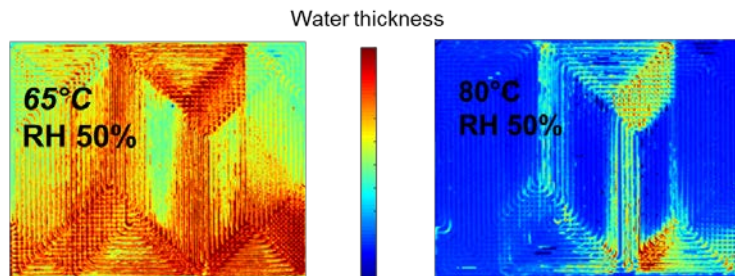
Measurement of the local current



Characterization of the local electrochemistry performances

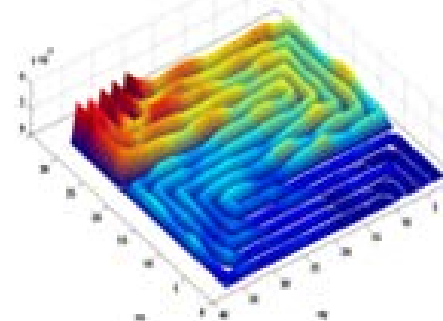


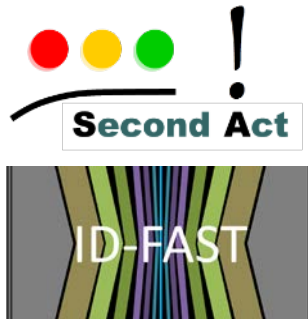
Measurement of the local water content



Neutron imaging on a reference stack
(Cf. E. Tardy)

Simulation of the local conditions and performances





Part of the research leading to these results has received funding from the European Union's Seventh Framework Programme (FP7/2007-2013) for the Fuel Cells and Hydrogen Joint Technology Initiative under grant agreement n°621216 (SECOND ACT) & from the Fuel Cells and Hydrogen 2 Joint Undertaking under the European Union's Horizon 2020 research and innovation program under grant agreement No. 779565 (ID-FAST).

Thank you!